Supporting Information

Achieving highly selective electrocatalytic CO_2 reduction by tuning CuO-Sb_2O_3 nanocomposites

Yangmei Li,[a] Senlin Chu,[a] Huidong Shen,[a] Qineng Xia,[*b] Alex W. Robertson,[*c] Justus Masa,[d] Umer Siddiqui[a] and Zhenyu Sun*[a]

[a] State Key Laboratory of Organic–Inorganic Composites, Beijing University of Chemical Technology, Beijing 100029, P. R. China

[b] College of Biological, Chemical Science and Engineering, Jiaxing University, Jiaxing 314001, Zhejiang, P. R. China

[c] Department of Materials, University of Oxford, Oxford, OX1 3PH, UK

[d] Analytische Chemie-Elektroanalytik & Sensorik, Ruhr-University Bochum, D-44780 Bochum, Germany

Corresponding author e-mail address: sunzy@mail.buct.edu.cn; xiaqineng@mail.zjxu.edu.cn; alex.w.robertson@gmail.com.

The Supporting Information contains:

Number of pages: 9

Number of figures: 5

Number of tables: 3

EXPERIMENTAL

Materials and reagents. All chemicals used in this work were of analytical grade and used as supplied. $Cu(Ac)_2{\cdot}H_2O$, $SbCl_3$, $Cd(NO_3)_2{\cdot}4H_2O$, $ZrCl_4$, and KOH were obtained from Aladdin. $Bi(NO_3)_3$ was purchased from Macklin. High-purity (≥95%) carbon black (CB) was supplied by Bayer Material Science.

Synthesis of CuO-metal oxide/CB catalysts. In a typical procedure to prepare CuO-Sb_2O_3/CB, a specific amount of $Cu(Ac)_2{\cdot}H_2O$ and $SbCl_3$ ethanol solutions (Table S1) were first mixed with 8 mg of CB dispersed in 8 mL of ethanol and bath-sonicated for 1 h to form a uniform dispersion. Different amounts of 0.5 M KOH ethanol solution (Table S1) were then slowly added into the mixture under vigorous magnetic stirring to ensure an appropriate pH value for the reaction system. The system was allowed to react for 6 h in an oil bath at 80 °C. After reaction, the solid products were repeatedly washed with ethanol and water, and then dried at 60 °C for use. Similarly, other metal oxide composite catalysts, such as CuO-CdO/CB, CuO-Bi_2O_3/CB, and CuO-ZrO_2/CB, were also synthesized by using corresponding metal precursors.

Characterization. X-ray powder diffraction (XRD) was performed with a D/MAX–RC diffractometer operated at 30 kV and 100 mA with Cu Kα radiation. X-ray photoelectron spectroscopy (XPS) experiments were carried out using Thermo Scientific ESCALAB 250Xi instrument. The instrument was equipped with an electron flood and a scanning ion gun. All spectra were calibrated according to the C 1s binding energy at 284.8 eV. HAADF-STEM was conducted using a JEOL ARM200 microscope with a 200 kV accelerating voltage. STEM samples were prepared by depositing a droplet of suspension onto a Cu grid coated with a Lacey Carbon film. Hydrogen temperature-programmed reduction (H_2-TPR) experiments were carried out in a quartz tube reactor equipped with a thermal conductivity detector (TCD) using a Micromeritics AutoChem HP 2950 instrument. Before each measurement, the sample was first pre-treated in pure Ar at 200 °C for 30 min. Subsequently, a certain amount of the pre-treated sample was heated in a gas flow (50 cm^3/min) of 10% H_2 in Ar from 50 to 750 °C at a ramp rate of 10 °C/min.

Cathode preparation. Typically, 1.2 mg of a catalyst was dispersed in 241.2 μL of solution containing isopropanol, deionized water, and 5 wt% Nafion solution with a corresponding volume ratio of 120: 120: 1.2 by ultrasonicating for 30 min to form a homogeneous ink. The catalyst ink was then loaded onto a carbon paper electrode with an area of 1.2 cm × 1 cm and dried under ambient conditions. For linear sweep voltammograms in Ar- or CO_2-saturated 0.1 M $KHCO_3$ solution, 1 mg of a catalyst was dispersed in the mixture of 100 μL of ethanol, 100 μL of deionized water, and 100 μL of Nafion solution (1 wt%). Then the mixture was ultrasonicated for 30 min to form a homogeneous ink. 7.95 μL of the dispersion ink was then loaded onto glassy carbon electrode and dried under ambient conditions.

Electrochemical measurements. For electrochemical reduction of CO_2, catalyst suspensions formed by dispersing 1.2 mg of the catalyst in 240 μL of IPA/H_2O (vol/vol 1:1) and 1.2 μL of 5% Nafion solution were deposited on carbon paper working electrodes to form catalyst films with a loading of 1 mg cm^{-2}. The formed

films were left to dry in the open air for 30 min. Cyclic voltammograms and linear scan voltammograms were recorded using glassy carbon working electrode in a three-electrode cell. Controlled potential electrolysis of CO_2 was tested in an H-cell system, which was separated by Nafion 117 membrane. Toray Carbon fiber paper with a size of 1 cm × 1 cm was used as working electrode. Pt wire and Ag/AgCl electrodes were used as counter electrode and reference electrode, respectively. The potentials were controlled by an electrochemical working station (CHI 760E, Shanghai CH Instruments Co., China). All potentials in this study were measured against the Ag/AgCl reference electrode (in 3 M KCl solution) and converted to the RHE reference scale by

E (*vs*. RHE) = E (*vs*. Ag/AgCl) + 0.21 V + 0.0591 × pH (Eq. S1)

Electrocatalytic reduction of CO_2 was performed in CO_2-saturated 0.1 M aqueous $KHCO_3$ at room temperature and atmospheric pressure. CO_2 with a flow rate of 10 mL min^{-1} was purged into the $KHCO_3$ solution for at least 30 min to remove residual air in the reservoir, then controlled potential electrolysis was conducted at each potential for 60 min.

Linear sweep voltammograms in Ar- or CO_2- atmosphere were carried out in a three-electrode system using Ag/AgCl as reference electrode, Pt wire as counter electrode, and glassy carbon as working electrode on a CHI 760E potentiostat (CHI 760E, Shanghai CH Instruments Co., China). Rotating disk electrode (RDE) experiments were run on an AFMSRCE RDE control system (Pine Inc., USA). The electrolyte is 0.1 M $KHCO_3$ solution with Ar or CO_2 purged for at least 30 min.

Faradaic efficiency (FE) measurement. Gas products: the FE values of catalysts were calculated using $\mathrm{FE} = \frac{Z * n * F}{Q_{total}}$ (Eq. S2), where Z is the number of electrons transferred (Z = 2 for CO and H_2 production), n the number of moles for a given product, F Faraday's constant (96485 C mol^{-1}), Q_{total} all the charge passed throughout the electrolysis process (measured by calculating the curve area of current density *vs*. time plot). CO and H_2 mole fractions of injected samples were calculated based on GC calibration curve. Liquid products: the FE values of catalysts were calculated using $\mathrm{FE} = \frac{\alpha * n * F}{Q}$ (Eq. S3), where α is the number of electrons transferred to form desired product (e.g., α = 2 for reduction of CO_2 to HCOOH), n is the number of moles for a desired product, F is the Faraday constant (96485 C·mol^{-1}), Q represents all the charge passed during a given time.

Partial current density determination. Partial current density for CO, HCOOH or H_2 can be obtained by multiplying corresponding FE by the total current density (J):

$J_{CO,\ HCOOH\ or\ H_2} = J \times \mathrm{FE}_{CO,\ HCOOH\ or\ H_2}$ (Eq. S4)

Number of active sites and turnover frequency (TOF) measurements. The TOF for CO formation was calculated as follows:

TOF (h^{-1}) = $[(J_{CO} \times S/Z^*F)/(m_{cat.} \times \omega/M)] \times 3600$ (Eq.

S5)

where J_{CO} is CO partial current (A cm^{-2}), S is the geometric surface area of working electrode (cm^2), Z is the number of electrons transferred (Z = 2 for CO formation), F is Faraday's constant (96485 C mol^{-1}), $m_{cat.}$ is catalyst mass in the electrode (g), ω is metal loading in the catalyst, M is atomic mass of metal (g mol^{-1}).

Product analysis of electrochemical CO_2 reduction reaction. Gas-phase analysis of the products of the electrochemical experiments was carried out using an Agilent 7890B GC system. Two thermal conductivity detectors and a flame ionization detector were used to analyze and differentiate the analytes. To characterize the gas product, 20 mL of produced gas in the dead volume of a gas bag (~ 2 L) was injected into the GC at identical experimental conditions e.g., pressure, temperature, and time using a sample lock syringe. CO and H_2 peaks were detected at a retention time of 11.4 and 3.7 min, respectively. The liquid product was analyzed in DMSO-d6 with tetramethylsilane (TMS) as an internal standard by ^1H nuclear magnetic resonance (NMR) (Bruker Avance III 400 HD spectrometer).

Table S1. The recipes for synthesizing the CuO-Sb_2O_3/CB materials.

Cu/Sb molar ratio	**CuO**	**~30:1**	**~20:1**	**~10:1**	**~5:1**	**~1:1**	**~1:5**	**Sb_2O_3**
N_{SbCl_3}/μmol	0	9.43	13.75	25.38	43.98	106.31	148.38	164.67
m_{SbCl_3}/mg	0	2.15	3.14	5.79	10.03	24.25	33.84	37.56
$N_{Cu(OAc)_2}$/μmol	300.00	282.82	274.95	253.77	219.88	106.31	29.68	0
$m_{Cu(OAc)_2}$/mg	59.90	56.47	54.89	50.66	43.90	21.23	5.92	0
C_{SbCl_3}/M				0.05				
V_{SbCl_3}/μL	0	189	275	508	880	2126	2967	3293
$C_{Cu(OAc)_2}$/M				0.05				
$V_{Cu(OAc)_2}$/μL	6000	5656	5499	5075	4397	2126	594	0
C_{CB}/mg/mL				1				
V_{CB}/mL				8				
C_{KOH}/M				0.5				
V_{KOH}/μL	800	800	800	800	800	800	800	800

Table S2. The ECR activity optimized by modulating the concentration and feeding sequence of the metal salt precursors.

$C_{metal\ salt\ precursors}$/M	**FE_{CO}/%**	**Feeding sequence of metal salt precursors**	**FE_{CO}/%**

0.005	65.4	Sb_2O_3@CuO/CB	71.9
0.01	90.0	Sb_2O_3-CuO/CB	90.0
0.02	62.5	CuO@Sb_2O_3/CB	70.2

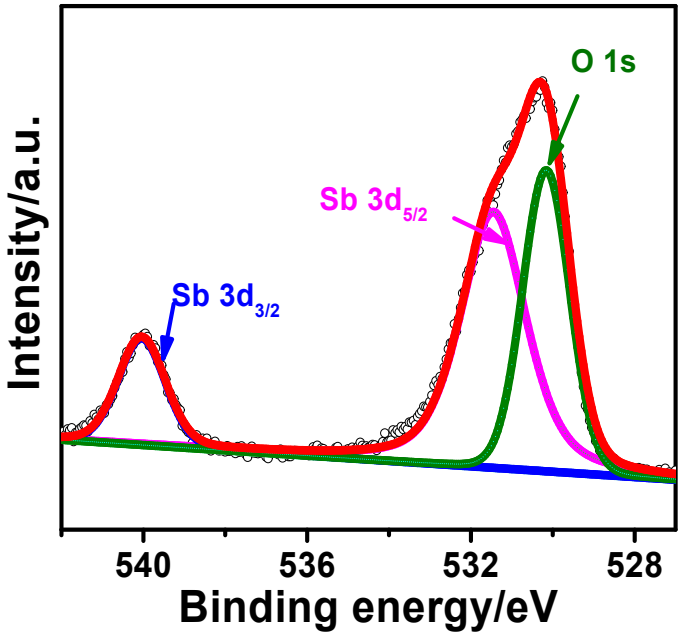

Figure S1. Sb 3d and O 1s XPS spectra of CuO-Sb_2O_3/CB (Cu-to-Sb mole ratio of 10:1).

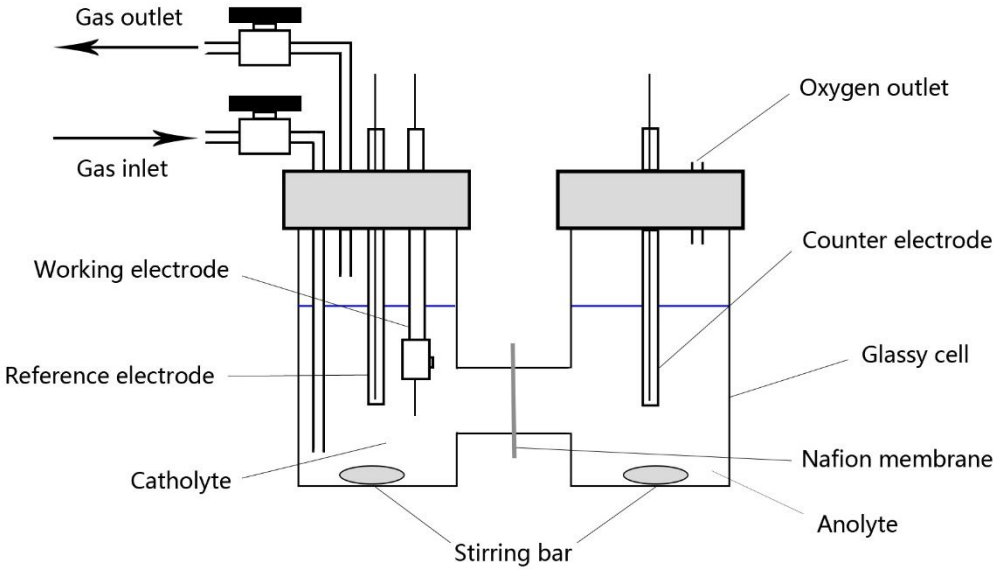

Figure S2. Illustration of an H-type cell for ECR.

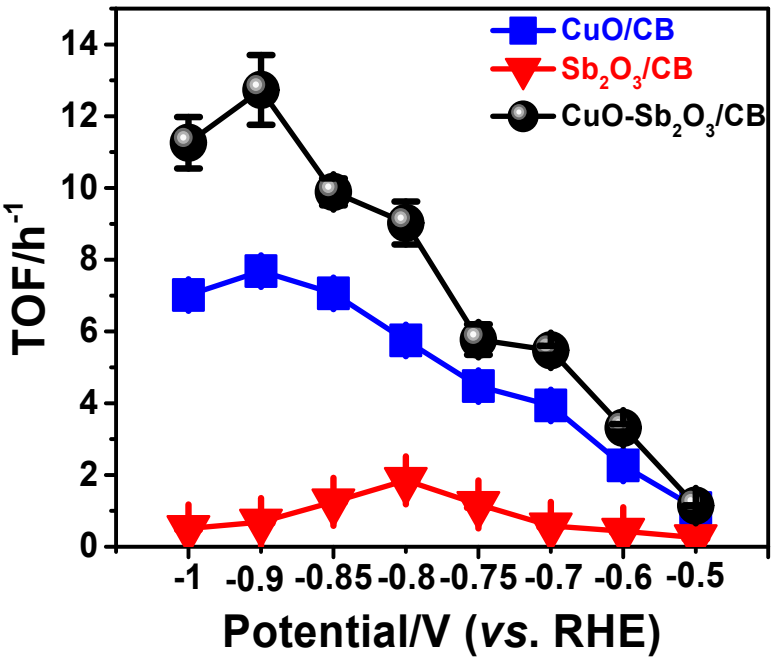

Figure S3. TOF plotted against applied potential over CuO/CB, Sb_2O_3/CB, and CuO-Sb_2O_3/CB.

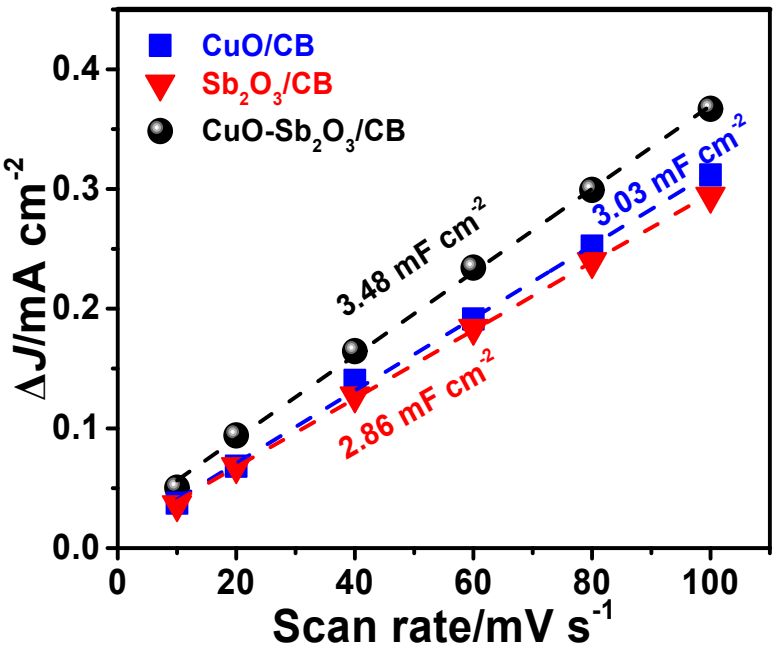

Figure S4. Charge current density difference versus scan rate for CuO/CB, Sb_2O_3/CB, and CuO-Sb_2O_3/CB.

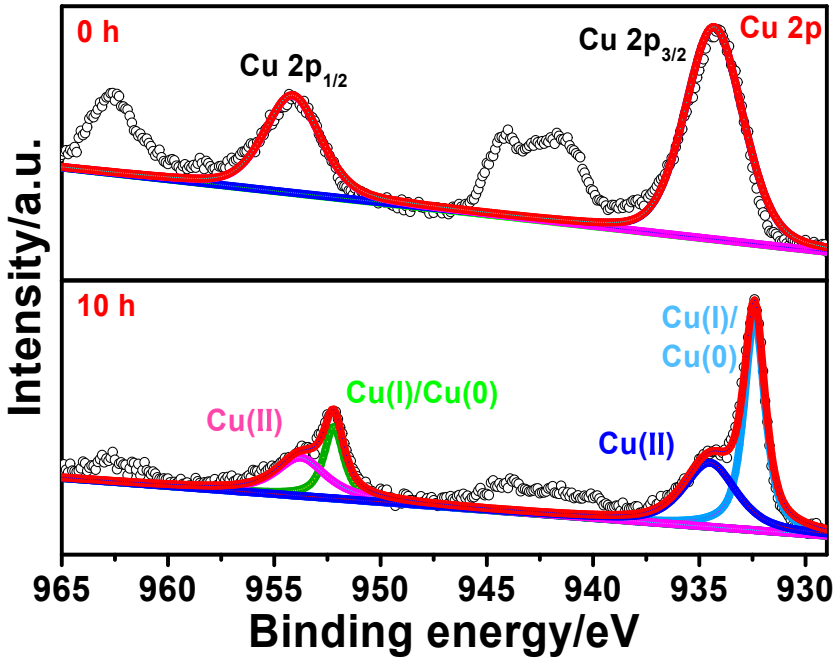

Figure S5. Cu 2p XPS spectra of CuO-Sb_2O_3/CB (Cu-to-Sb mole ratio of 10:1) before (top panel) and after 10 h of continuous electrolysis (bottom panel).

Table S3. Summary of the reported ECR electrocatalysts shown in Fig. 5a.

Catalyst	**Electrolyte**	**Potential/V (*vs.* RHE)**	**CO partial current density/mA cm^{-2}**	**CO FE (%)**	**Ref.**
CuO-Sb_2O_3/CB	0.1 M $KHCO_3$	−0.8	4.35	90.0	This work
Cu/Au	0.1 M $KHCO_3$	−1.0	5.21	58.0	1
$CuAu_3$	0.1 M $KHCO_3$	−0.72	2.8	64.7	2
CuIn-Act	0.5 M $KHCO_3$	−0.6	2.66	68.2	3
$Cu_{0.2}Zn_{0.4}Sn_{0.4}$	0.1 M $KHCO_3$	−0.4	2.8	86.0	4
Cu/SnO_x-CNT	0.1 M $KHCO_3$	−0.99	11.3	89.0	5
Cu-Pd	0.1 M $KHCO_3$	−0.9	3.4	87.0	6
ZnO	0.1 M $KHCO_3$	−1.1	16.1	83.0	7
Ag-Sn	0.5 M $NaHCO_3$	−1.1	5.1	80.0	8
Fe/NC	0.1 M $KHCO_3$	−0.6	1.7	80.0	9
Ag_{600}/In/CF	0.5 M $KHCO_3$	−0.53	1.4	77.4	10
Cu nanowires	0.1 M $KHCO_3$	−0.4	1.81	62.0	11
Ag@Cu NPs	0.1 M $KHCO_3$	−1.06	1.75	82.0	12
Sn/Cu	0.1 M $KHCO_3$	−0.9	18.75	80	13
$Ag_{84}Cu_{16}$	0.5 M $KHCO_3$	−0.7	2.63	43.9	14

$CuInO_2$	0.1 M $KHCO_3$	−0.8	1.67	70	15

References

(1) Kim, J. H.; Woo, H.; Yun, S. W.; Jung, H. W.; Back, S. Highly active and selective Au thin layer on Cu polycrystalline surface prepared by galvanic displacement for the electrochemical reduction of CO_2 to CO. *Appl. Catal. B Environ.* **2017**, *213*, 211–215, DOI org/10.1016/j.apcatb.2017.05.001.

(2) Kim, D.; Resasco, J.; Yu, Y.; Asiri, A. M.; Yang, P. D. Synergistic geometric and electronic effects for electrochemical reduction of carbon dioxide using gold–copper bimetallic nanoparticles. *Nat. Commun.* **2014**, 5, 4948, DOI 10.1038/ncomms5948.

(3) Janga, Y. J.; Leeb , J.; Kima, J. H.; Leea, B. J.; Lee, J. S. One-dimensional CuIn alloy nanowires as a robust and efficient electrocatalyst for selective CO_2-to-CO conversion. *J. Power Sources* **2018**, *378*, 412–417, DOI org/10.1016/j.jpowsour.2017.12.070.

(4) He, J. F.; Dettelbach, K. E.; Huang, A. X.; Berlinguette, C. P. Brass and bronze as effective CO_2 reduction electrocatalysts. *Angew. Chem. Int. Ed.* **2017**, *129*, 16806–16809, DOI 10.1002/ange.201709932.

(5) Huo, S. J.; Weng, Z.; Wu, Z. S.; Zhong, Y. R.; Wu, Y. S.; Fang, J. H.; Wang, H. L. Coupled metal/oxide catalysts with tunable product selectivity for electrocatalytic CO_2 reduction. *ACS Appl. Mater. Interfaces* **2017**, *9*, 28519–28526, DOI 10.1021/acsami.7b07707.

(6) Mun,Y. D.; Lee, S.; Cho, A.; Kim, S.; Han, J. W.; Lee, J. Cu-Pd alloy nanoparticles as highly selective catalysts for efficient electrochemical reduction of CO_2 to CO. *Appl. Catal. B Environ.* **2019**, *246*, 82–88, DOI org/10.1016/j.apcatb.2019.01.021.

(7) Geng,Z. G.; Kong, X. D.; Chen, W. W.; Su, H. Y.; Liu, Y.; Cai, F.; Wang, G. X.; Zeng, J. Oxygen vacancies in ZnO nanosheets enhance CO_2 electrochemical reduction to CO. *Angew. Chem. Int. Ed.* **2018**, *57*, 6054–6059, DOI 10.1002/ange.201711255.

(8) Luc, W. W.; Collins, C.; Wang, S.; Xin, H. L.; He, K.; Kang, Y. J.; Jiao, F. Ag-Sn bimetallic catalyst with a core-shell structure for CO_2 reduction. *J. Am. Chem. Soc.* **2017**, *5*, *139*, DOI 10.1021/jacs.6b10435.

(9) Zhang, C. H.; Yang, S. Z.; Wu, J. J.; Liu, M. J.; Yazdi, S.; Ren, M. Q.; Sha, J. W.; Zhong, J.; Nie, K. Q.; Jalilov, A. S.; Li, Z. Y.; Li, H. M.; Yakobson, B. I.; Wu, Q.; Ringe, E.; Xu, H.; Ajayan, P. M.; Tour, J. M. Electrochemical CO_2 reduction with atomic iron-dispersed on nitrogen-doped graphene. *Adv. Energy Mater.* **2018**, 1703487, DOI org/10.1002/aenm.201703487.

(10) Lee, H.; Kim, J.; Choi, Insoo; Ahn, S. H. Nanostructured Ag/In/Cu foam catalyst for electrochemical reduction of CO_2 to CO. *Electrochi. Acta* **2019**, *323*, 133102, DOI 10.1016/j.electacta.2018.11.101.

(11) Liang, C.; David, R.; Li, C. Y.; Livi, J. T.; Rottmann, P. F.; Hemker, K. J.; Mueller, T.; Wang, C. Mechanistic insights for low-overpotential electroreduction of CO_2 to CO on copper nanowires. *ACS Catal.* **2017**, *7*, 8578–8587, DOI 10.1021/acscatal.7b03107.

(12) Chang, Z. Y.; Huo, S. J.; Zhang, W.; Fang, J. H.; Wang, H. L. The Tunable and Highly Selective Reduction Products on Ag@Cu Bimetallic Catalysts Toward CO_2 Electrochemical Reduction Reaction. *J. Phys. Chem. C* **2017**, *121*, 11368–11379, DOI 10.1021/acs.jpcc.7b01586.

(13) Ju, W. B.; Jiang, F. Z.; Ma, H.; Pan, Z. Y.; Zhao, Y. B.; Pagani, F.; Rentsch, D.; Wang, J.; Battaglia, C. Electrocatalytic Reduction of Gaseous CO_2 to CO on Sn/Cu-Nanofber-Based Gas Diffusion Electrodes. *Adv. Energy Mater.* **2019**, 1901514, DOI 10.1002/aenm.201901514.

(14) Choi, J. H.; Kim, M. J.; Ahn, S. H.; Choi, I.; Jang, J. H.; Ham, Y. S.; Kim, J.; Kim, S, K. Electrochemical CO_2 reduction to CO on dendritic Ag-Cu electrocatalysts prepared by electrodeposition. *Chem. Eng. J.* **2016,** *299*, 37–44, DOI org/10.1016/j.cej.2016.04.037.

(15) Jedidi, A.; Rasul, S.; Masih, D.; Cavalloa, L.; Takanabea, K. Generation of Cu-In alloy surfaces from $CuInO_2$ as selective catalytic sites for CO_2 electroreduction. *J. Mater. Chem. A* **2015**, *3*, 19085–19092, DOI 10.1039/c5ta05669a.